International Journal of Future Engineering Innovations

The Effects of Welding Parameters on The Integrity and Structure of HSLA Pipeline Steel Butt Fusion Welds

Onotu Charles [1], Ihom AP [2*], Odeh EU [3], Markson IE [4]
[1-4] Department of Mechanical and Aerospace Engineering, Faculty of Engineering, University of Uyo, PMB 1017 Uyo, Akwa Ibom State-Nigeria

* Corresponding Author: **Ihom AP**

Article Info

ISSN (online): 3049-1215
Impact Factor (RSIF): 8.25
Volume: 03
Issue: 02
March-April 2026
Received: 09-01-2026
Accepted: 07-02-2026
Published: 05-03-2026
Page No: 31-43

Abstract
High-Strength Low-Alloy (HSLA) steel is a preferred material for pipeline construction due to its high strength, toughness, and resistance to environmental degradation. However, welding HSLA steel introduces significant challenges, particularly concerning the structural integrity, mechanical performance, and long-term durability of butt-fusion welds. The welding process produces fusion and heat-affected zones with microstructures that differ significantly from the parent material, often leading to graded structures, residual stresses, hardness variations, and susceptibility to brittle fracture or corrosion. This study investigates the influence of key welding parameters—including heat input, welding sequence, weld bead geometry, and post-weld heat treatment (PWHT)—on the microstructure, mechanical properties, and corrosion behaviour of HSLA pipeline steel butt-fusion welds. A series of controlled experiments were conducted in which standard butt-weld joints were fabricated under varying welding conditions. Tensile testing revealed that the base HSLA steel had an ultimate tensile strength of 426.62 MPa, yield strength of 404.27 MPa, and elongation at break of 32.5%. Optimized welded joints exhibited improved ultimate tensile strength of approximately 460 MPa. Impact toughness more than doubled, increasing from 30.4 J in the untreated material to 75.78 J in PWHT-treated welds. Hardness measurements indicated peak values of 653.3 HV in high-hardness HAZ regions, which decreased to 310.3 HV after PWHT, balancing strength with ductility. Electrochemical corrosion testing demonstrated that PWHT improved performance, with open circuit potential shifting from −0.58 V to −0.21 V and current density reducing from 2.2×10^{-4} A/cm² to 1.0×10^{-4} A/cm². Microstructural analysis confirmed the transition from ferrite–pearlite in the base material to acicular ferrite in the as-welded HAZ and tempered martensite after PWHT. Multi-response optimization using Taguchi signal-to-noise ratios and Grey Relational Analysis identified the optimal welding condition as Experiment 25 of the L25 Taguchi array, combining a 180 A welding current, 26 V arc voltage, 140 mm/min travel speed, and a heat input of approximately 1.8 kJ/mm, achieving a Grey Relational Grade of ~0.88. The results demonstrate that controlled heat input, appropriate multi-pass welding sequences, and effective post-weld heat treatment are essential for achieving HSLA welds with balanced mechanical properties, reduced susceptibility to cracking, and improved corrosion resistance. This study provides quantitative guidance for pipeline welding, enabling safer, more reliable, and cost-efficient fabrication while advancing the understanding of how welding parameters influence the microstructure and performance of HSLA steel butt-fusion welds. The findings are directly applicable to industrial pipeline fabrication and have implications for optimizing welding practices to prevent joint failure in service.

DOI: https://doi.org/10.54660/IJFEI.2026.3.2.31-43

Keywords: High Strength Low Alloy, Steel, Welds, Properties, Microstructure, Integrity, Pipelines

1. Introduction

In Nigeria, the oil and gas sector account for about 35% of the country's GDP, while petroleum export earnings account for more than 90% of overall export revenue. Nigeria's other natural resources, in addition to petroleum, include natural gas, tin, iron ore, coal, limestone, niobium, lead, zinc, and arable land. Nigeria has one of the world's ten biggest natural gas reserves, with about half of the resources discovered in conjunction with oil. It possesses the largest deposits of natural gas in Africa, most of which are located in and around the Niger Delta region (Lindén and Pålsson, 2013) [19]. This natural gas is available in two forms: gas

from isolated wells (or non-associated gas) and gas discovered in conjunction with oil (associated gas). These two sources are present in nearly equal amounts. While non-associated gas may be left underground until needed, associated gas is unavoidably lifted together with crude oil from its reserve, and must either be recovered or disposed of on-site as an unwanted by-product of oil. The common on-site disposal methods are by venting, if the volume is small enough, or flaring for larger volumes (Ibitoye, 2014) [11].

Today, networks of pipeline systems are used to transport this natural gas over long distances in the Nigerian onshore/offshore oil and gas industries, as compared to other risky and unreliable means such as oil-gas tankers and tank trucks/railroad tank cars (Rehman and Nawaz, 2017) [24]. During the installation of the pipeline network system, welding is required to join one member to another, and weld defects have been identified as the major causes of pipeline failure (Chen, Xie, Wang and Li, 2022) [10]. Welding is a critical process in the fabrication of pipelines, particularly those constructed from High-Strength Low-Alloy (HSLA) steel. Welding parameters play a pivotal role in determining the integrity and performance of welded joints, influencing properties such as microstructure, mechanical strength, and corrosion resistance. Although nowadays welding is a mechanized process, it is still very reliant on highly skilled welders and procedure development. The procedure parameters are initially set but the welder typically must control the torch cross seam positioning, oscillation width, and contact tip to work distance (CTWD), as the torch progresses from the 12 o'clock position to the 6 o'clock position. As the torch systems evolved and the welding speeds increased, it became very hard for the welder to be able to cope, leading to weld defects (Yapp and Blackman, 2004) [25].

Adding to the increasing welding speed, for a large diameter pipe, a welder may be standing on top of a ladder for the weld start and laying on his back on the floor at the end of the weld. Welders visually inspect welds before and after welding, and if they detect asymmetric or convex welds, they will grind the affected area to produce a concave shape before they lay the next bead (Yin *et al*., 2022) [26]. However, due to a large number of filling layers, the probability of defects is greatly increased which affects the integrity of the long-diameter oil and gas pipeline network systems.

Given the growth in pipeline installations all over the world, and constant expansion in natural gas consumption in Nigeria today, the need for reliable fusion welding parameters has become increasingly important to ensure long-term pipeline fitness-for-service performance. The effects of fusion welding on HSLA steel pipes have been summarized in many studies (Haribalaji, Boopathi and Balamurugan, 2014; Ragu, Balasubramanian, Malarvizhi and Rao, 2015; Miletić *et al*., 2020) [23, 23, 21]. The microstructure and mechanical properties of the S-series welded HSLA steels had mostly been studied with little emphasis on their corrosion behaviour in a typical oilfield environment. It has been noted that welds in these hardened high-strength grades of steel can be susceptible to preferential corrosion when buried, so in regions where loss of coating may occur through abrasion, impact or wear, additional effort will be needed to ensure preferential corrosion will not take place. Welding influences material properties, and so must be considered in terms of design and initial fabrication and any subsequent repair during the operational life of the transmission pipeline to predict the acceptable corrosion service life of the welded structure (Mičian, Frátrik and Kajánek, 2021; Osoba, Ayoola, Adegbuji and Ajibade, 2021) [20, 22].

The oil and gas industry in Nigeria will be one of the key industries demanding extensive pipe welding due to the prediction of a doubling of natural gas consumption over the next 20 years (Harris, 2011). With this increase in demand, more of the oil and gas transmission pipelines will be installed via welding. Welds in pipes exhibit special microstructural and compositional features due to the thermal cycle of heating and cooling which occur during the welding process. These pipelines, manufactured by welded segments of shielded metal arc welding (SMAW), can be divided into three distinct zones known as the weld bead (WB), the heat-affected zone (HAZ), and the base metal (BM) due to heat input during the welding process. These regions differ in microstructure, chemical composition and residual stress level. Preferential weld corrosion can be galvanically induced, or related to the microstructure associated with the HAZ and weld metal.

This research aimed to investigate the impact of welding parameters on the microstructure, mechanical properties, and corrosion behaviour of HSLA pipeline steel butt-fusion welds. By systematically exploring these factors, the study sought to contribute to the optimization and enhancement of weld joint integrity in HSLA steel pipelines.

2. Materials and Method

2.1. Materials and Equipment

The materials and equipment used for the study include a turret Lathe, API 5LX series of HSLA steel pipes, welding electrodes, heat treatment furnace, corrosion testing devices, scanning electron microscope (SEM), optical emission spectrometer (OES), computer and computer software, electronic weighing balance, 100% duty cycle SMAW machines, and MIG welding machine. Also used were the hacksaw, universal strength testing machine, impact testing machine, Vickers hardness tester, wear tester, filing machine, and weld gauge (MG-8 Cam type gauge – to determine undercut, excess weld metal (capping size) and misalignment).

2.2. Method

The experimental study for the proposed study began just after the theoretical information was gathered. The API 5LX series of HSLA steel with known thickness and dimensions were prepared for the experiment. About 30% of the prepared samples were subjected to destructive tests for weld quality acceptance. Before the post-weld heat treatment (PWHT), as-welded samples were mechanically shot blasted, chemically cleaned and analysed. The SMAW and MIG arc welding machines were used to manufacture the butt fusion welded specimens according to the BS, API, and AS/NZS standard specifications. Microstructural analysis of the various zones of the welded API 5L X series were carried out. The as-welded specimens were code-named for ease of identification. The results of the samples were tabulated and computed to determine the effect of arc welding parameters on the weld quality of the studied HSLA steel materials. Optimization analysis was carried out to know the best combination of welding parameters for quality weld and predictive models were developed using the results of the tests. This was done using computer software. The laboratory accelerated corrosion immersion test and electrochemical

impedance spectroscopy (EIS) measurements were adopted to evaluate the corrosion behaviour of the as-welded HSLA steel samples in a typical oilfield corrosion environment.

Joint Preparation

The researcher prepared and welded the samples in line with the API 1104 guidelines and details of dimensions for butt weld joint design, with included groove angle of 60° of single-V butt-joints for investigation. Figure 2.1 show the preparation of the HSLA test specimens on the lathe machine.

Fig 1: Preparation of the HSLA sample material on a lathe

Welding of Test Samples

Current welding standards and procedures such as API 1104, AS/NZS 1554.4, CAN/CSA-Z662-15, and BS 2633, were used for welding the test specimens, these standards provide guidelines on butt fusion welding of oil and gas pipelines. Figures 2.2-2.4 show Cut sections of the pipe material before welding, two sections of the HSLA sample material tacked together before root pass welding, and sample material welded in 6G position after hot pass welding.

Fig 2: Cut sections of the pipe material before welding

Fig 3: Two sections of the HSLA sample material tacked together before root pass welding

Fig 4: Sample material welded in 6G position after hot pass welding

Weld Quality Test of Samples

A tension test and impact test were carried to determine the weld's ultimate strength and degrees of weld toughness. The Cross-Tension Test and U-Tension Test were applied on the samples, while for the impact test of samples, the Shear-Impact Test, Drop-Impact Test, Shear-Impact Loading Test, and Tension-Impact Loading Test were applied. Figure 3.5 show HSLA Samples for Mechanical tests after welding, cutting, and PWHT.

Fig 5: HSLA Samples for Mechanical tests after welding, cutting and PWHT

Post-Weld Heat Treatment of Test Samples

A representative butt-fusion weld samples fabricated with relevant welding parameters was selected for investigation. Three different holding temperatures (600 °C, 570 °C and 540 °C) and three holding times (0.5, 1, and 3 hrs.) recommended for the corresponding holding temperatures was applied for the specimens. To carry out the heat treatment task, a muffle heating furnace with a maximum heating capacity of 1200 °C and robust refractory bricks inside was employed to simulate the thermal cycles of PWHT. The internal dimensions (width × depth × height) of the oven was 500 × 500 × 700 mm large enough to accommodate the specimens.

During heat treatment, a laser (non-contact) temperature measuring device was used to determine the sample temperature in the weld zone, heat affected zone and unwelded zone. The samples were preheated to gradually raise their temperature to a predetermined level as this will prevent thermal shock during the main heat treatment. The temperature of the furnace was increased to the desired PWHT temperature and held at this temperature for the specified soaking time. After the soaking time is complete, the heat-treated samples (heated below the subcritical temperature) were cooled using a recommended controlled-cooling rates as specified in guidelines. Figure 2.6 show the Muffle Furnace used for PWHT.

Fig 6: The Muffle Furnace used in PWHT

Characterization of Test Samples

Prior to corrosion testing, the three distinct zones (heat-affected zone, weld bead and base metal) of the as-welded and heat-treated samples was subjected to microstructure and chemical composition analysis. Optical microscope (OM) and Scanning electron microscope (SEM) equipped with energy dispersive spectrometer (EDS) and wavelength-dispersive spectrometer (WDS) was used for microstructure analysis, while the chemical composition was analysed using an Optical emission spectrometer (OES) equipped with photoelectric photometry. This was done by exposing the well-polished surface of the samples to light emission from the spectrometer. The microstructure, elements contained, and their proportions were revealed on the digital processor attached to the spectrometer.

Metallographic Inspection

To understand the effect of welding on microstructural variations, welded specimens were sectioned and mirror polished utilizing diamond suspensions (6µm to 0.25µm) following ASTM E3-11 standard (ASTM-International 2011). Polished specimens were then chemically etched according to ASTM E407-07 standard (ASTM-International 2007) to reveal the constituents and microstructures. Different metals and alloys required different types of etchants. In this study, about 2% Nital solution was utilized for the studied steels. The Nital (2%) solutions comprised 2 mL HNO_3 and 98 mL ethyl alcohol. The chemically etched specimens were thereafter inspected under a metallographic digital light optical microscope (OM) and scanning electron microscope (SEM) to obtain micrographs. Fracture surfaces of the tensile tested specimens were analysed with a Quanta 3D FEG scanning electron microscope (SEM) to understand the microstructural and fracture behaviour of the fusion welded butt joints.

Elemental Chemical Composition

The quantitative elemental chemical compositions of the weldment (WB), heat affected zones (HAZ), and base metal (BM) of the samples were evaluated using a JEOL 6390 LV scanning electron microscope (SEM) equipped with a PGT PRISM IG (intrinsic Ge) energy dispersive X-ray (EDX) spectroscopy detector

Mechanical Properties of Butt-Welded Samples

Tensile Test

Determining weld tensile strength by tensile testing is a weld qualification requirement listed in ASME IX code case 2832 for fusion welding. The code case specifies that the tensile test "was done by removing two tensile test specimens", "with the weld area located in the centre, and the axis of the weld transverse to the width of each tensile test specimen", with "one face of each specimen common to the centre of the weld". The tensile test samples were prepared from the parent material, approximately 300 mm from the weld for reference purposes. After preparation, the samples were surface ground on both faces to a 3 mm thickness to remove any residual surface effect or wire cutting line marks which may negatively influence the performance or act as a stress raiser during sample evaluation. The butt fusion welded samples were lightly etched to identify the weld location before machining the dog-bone shape. The ASME IX Code Case 2832 specifies samples to be machined according to QW-462.1. The specimens complied with all dimensional requirements.

Impact Tests

Impact testing was used to estimate the fracture toughness of the as-welded and heat-treated samples. In this measurement, a weighted striker impacts a notched specimen. The tests measure the total energy absorbed in fracture. Several data points of fracture energy were obtained by varying the depth of the notch.

Hardness Test

Due to the fine scale of the various microstructures in the dissimilar weld fusion zone, nanoindentation testing was selected, to measure the variation in hardness across the steel–buttering interfaces. A Micromaterials Nanotester, equipped with a Berkovich tip, was used at room temperature to determine the hardness of the samples. Arrays of 10 x 10 indents, angled acutely across the interface was used which will provide a high point-to-point resolution. The test specimens were cut from the butt fusion joint with the weld bead intact and at the centre. The cuts were made at low speeds to mitigate induced heating of the samples before polishing the cut surfaces. These specimens, measuring 25 mm by 25 mm was machined to ensure that the indentation surface is parallel to the back of the specimen.

The test surfaces of each specimen were ground and polished with successively finer grades of abrasive silicon carbide paper to achieve an average surface roughness of 2.5 µm before testing the specimen. Several nanoindentation trials were conducted to establish suitable test parameters to investigate the variation in material properties across the weld interface. The Berkovich indenter was selected due to its conformity arising from its simple 3-sided shape. A grid of 60 columns by 3 rows of indents, spaced 100 µm apart, justified over the weld interface at the centre of the pipe wall thickness was used for each specimen. The nanoindenter required the operator to calibrate the distance between the indenter and the specimen surface after every millimetre of indents to ensure the accuracy of the indentations.

Electrochemical Corrosion Measurements

Evaluation of the corrosion behaviour of the as-welded and heat-treated butt fusion weld joints was carried out using an accelerated corrosion test method that meets the ASTM industrial standards. The HSLA pipeline steel materials were obtained from Harmony Steel and Construction Co. Ltd. Port Harcourt in the form of a sheet. Circular specimens of about 38 mm (1.5-in.) diameter with a thickness of approximately 3 mm (0.125-in.) and an 8-mm (5⁄16-in.) diameter hole for mounting was prepared for the experiment. The total surface area of samples for corrosion evaluation was determined and

recorded. Before corrosion testing, the prepared steel samples were shot and grit blasted to achieve a clean surface free of deleterious species that may negatively influence the corrosion data obtained during the experiment. Thereafter, the samples were degreased by pre-treating in acetone and ethanol solutions using ultrasonication and thoroughly washed with distilled water before exposure to the corrosion medium. Both the accelerated chemical corrosion test by total immersion and electrochemical corrosion analysis using electrochemical impedance spectroscopy (EIS) was adopted to evaluate the corrosion behaviour of the prepared samples.

Accelerated Chemical Corrosion Measurement

The corrosion behaviour of samples was evaluated in an accelerated corrosion test by total immersion at ambient temperatures in a typical 5000 mL resin flask having a reflux condenser with an atmospheric seal, a sparger for controlling atmosphere or aeration, a thermowell and temperature-regulating device, and a specimen support system according to the ASTM G 31 – 72 (2004) standards.

Electrochemical Corrosion Measurement

The electrochemical corrosion response of the prepared HSLA pipeline steel samples was probed in different electrolyte solutions using electrochemical impedance spectroscopy (EIS) using the Gamry Instrument's Interface 1000 Potentiostat/ZRA. The ASTM B457 – 67 (2003) standard test method was followed to evaluate the electrochemical corrosion behaviour of the samples.

Characterization of Corrosion Products

Localized Corrosion

NPFLEX 3D Surface Metrology made by Bruker was used to measure the pitting corrosion of the exposed as-welded HSLA steel samples. NPFLEX is designed specifically for investigating different sample sizes and shapes without damaging the sample.

Surface Scale Measurements

Surface appearance (topography): Scanning Electron Microscopy (SEM) was used to examine the surface appearance (topography) of the corrosion film formed after the samples were exposed to the various simulated oilfield environments. The SEM contains a metallic filament which is heated and produces an electron beam. The electron beam makes its way through electromagnetic lenses which focus and direct the beam onto the sample. Once it hits the sample, electrons are backscattered and secondary electrons are ejected from the sample. Detectors collect the electrons and convert them to a signal which is used to produce an image on a TV screen.

Elemental composition: Energy dispersive X-ray (EDX) was used to evaluate the elemental composition of the surface films formed on the steel specimen.

Predictive Model Development

To understand the influence of welding parameters on the properties of HSLA pipeline steel butt-fusion welds, a Taguchi–Grey Relational Analysis (Taguchi–GRA) framework was developed. Although linear regression and neural network techniques were initially considered during the conceptual stage of the research, the limited sample size and the need for robust multi-response optimization necessitated the adoption of the Taguchi–GRA method as the primary predictive and optimization tool.

Although classical Taguchi orthogonal arrays such as L9 are commonly used in literature, their direct application was not feasible in this work due to welding procedure qualification constraints, limited sample size, and the inclusion of post-weld heat treatment variables. Consequently, Taguchi signal-to-noise ratio analysis coupled with Grey Relational Analysis was adopted to enable robust multi-response optimization without reliance on a fixed orthogonal array.

Data Collection

A comprehensive dataset that includes information on the welding parameters (independent variables) used, as well as the corresponding weld properties (dependent variables) such as microstructure characteristics, mechanical properties, and corrosion behaviour was properly gathered. This dataset served as the foundation for the Taguchi-GRA analysis.

Control Factors

Key parameters that are likely to have a significant impact on the weld properties were identified. These process parameters include current, voltage, welding speed, heat input, welding sequence, and post-weld heat treatment conditions.

Taguchi-Grey Relational Analysis

The heat input equation for the welding of the HSLA samples for each condition is calculated and is given by Equation 3.3.

$$HI = \frac{V \times I}{S} \qquad \text{Equation 2.3}$$

Where:
HI = Heat input (kJ/mm)
V = Arc voltage (V)
I = Welding current (A)
S = Welding speed (mm/s)

In this study, an experimental design was developed and implemented in the Taguchi-Grey Relational analysis. Table 2.2 provides the experimental design implemented in the analytical study of the welding parameters.

Table 1: Experimental Design for Multi-Pass SMAW of HSLA Pipeline Steel

Welding Pass	Electrode Type	Current Range (A)	Arc Voltage (V)	Travel Speed (mm/min)	Heat Input (kJ/mm)
Root Pass	E6010	80–120	18–22	80–100	0.8–1.1
Hot Pass	E7018 (Low-H_2)	110–140	20–24	90–110	1.1–1.3
Filler Pass 1	E7018	130–160	22–26	100–120	1.3–1.6
Filler Pass 2	E7018	140–170	22–26	110–130	1.4–1.7
Cap Pass	E7018	150–180	22–26	120–140	1.5–1.8

Source: Researcher (2025)

Taguchi Signal-to-Noise (S/N) Ratios
The larger-the-better criterion was used for UTS and Impact Toughness. This is given by Equation 2.4. On the other hand, smaller-the-better criterion was used for assessing the corrosion density, i_{corr}. The smaller-the-better criterion is given by Equation 2.5. Furthermore, Equation 2.6 gives an expression of the nominal-the-best criterion, which is used in assessing hardness of the weld joint.

$$S/N_{LTB} = -10\log_{10}\left(\frac{1}{n}\sum_{i=1}^{n}\frac{1}{y_i{}^2}\right) \quad \text{Equation 2.4}$$

Where:
y_i = observed response value
n = number of repetitions
Also,

$$S/N_{STB} = -10\log_{10}\left(\frac{1}{n}\sum_{i=1}^{n}y_i{}^2\right) \quad \text{Equation 2.5}$$

Furthermore, nominal-the-best criterion,

$$S/N_{NTB} = 10\log_{10}\left(\frac{\mu^2}{\sigma^2}\right) \quad \text{Equation 2.6}$$

Where:
μ = target or mean value
σ = standard deviation
In this study the target hardness ≈ 600 HV. This criterion minimizes excessive hardness that may cause hydrogen-assisted cracking and reduce impact toughness.

Data Normalization (Grey Relational Analysis)
Normalization converts different response scales into a dimensionless range [0 1]. Data normalization was applied on larger-the-better, smaller-the-better and nominal-the-better criterion. Normalization of larger-the-better criteria is given by Equation 2.7.

$$x_i{}^* = \frac{x_i - max(x)}{max(x) - min(x)} \quad \text{Equation 2.7}$$

Equation 3.8 gives an expression for normalization of smaller-the-better criteria.

$$x_i{}^* = \frac{max(x) - x_i}{max(x) - min(x)} \quad \text{Equation 2.8}$$

Furthermore, Equation 2.9 is an expression for normalization of nominal-the-best criteria.

$$x_i{}^* = 1 - \frac{|x_i - x_0|}{max|x_i - x_0|} \quad \text{Equation 2.9}$$

Where:
x_0 = target value

The deviation of each normalized response from the ideal value (1) is computed as in Equation 3.10:

$$\Delta_i = |1 - x_i{}^*| \quad \text{Equation 2.10}$$

Grey Relational Coefficient (GRC)
The GRC quantifies the closeness of each experiment to the ideal condition.

$$\xi_i = \frac{\Delta_{min} + \zeta\Delta_{max}}{\Delta_i + \zeta\Delta_{max}} \quad \text{Equation 2.11}$$

Where:
$\Delta_{min} = \min(\Delta_i)$
$\Delta_{max} = \max(\Delta_i)$
ζ = distinguishing coefficient = 0.5

Grey Relational Grade (GRG)
The GRG represents the overall multi-response performance index.

$$GRG = \frac{1}{m}\sum_{j=1}^{m}\xi_{ij} \quad \text{Equation 2.12}$$

Where:
m = number of response characteristics
ξ_{ij} = GRC of response j for experiment i
In this study, as applied in computing the UTS, impact toughness, hardness and corrosion:

$$m = 4$$

The ranking of welding conditions was computed using Equation 2.13. Higher value of GRG implies better combined mechanical and corrosion performance.

$$Optimal\ Condition = max(GRG) \quad \text{Equation 2.13}$$

Statistical Validity Under Limited Samples
The Taguchi–GRA framework relies on the fact that process robustness is proportional to the S/N ratio. This thus validates inference made with small sample sizes and follows API 1104/ASME IX welding procedure qualification philosophy.

Metallurgical Optimization of the Weld Joint
The optimized welding parameters depend predominantly on the balanced heat input, controlled HAZ hardness, refined microstructure, improved toughness and corrosion resistance. Mathematically, this is expressed in Equation 2.14.

$$Optimal\ weld\ quality = f(HI, I, V, S, HT) \quad \text{Equation 2.14}$$

3. Results and Discussion

3.1. Tensile Properties of HSLA Steel (Control versus Welded Samples)

Before assessing the performance of the welded joints, tensile testing was carried out on the base HSLA steel in its untreated condition. This provided a reference point against which the effects of welding and post-weld treatments could be evaluated. The results of the control tensile tests are presented in Table 3.1.

Table 2: Tensile Properties of HSLA Steel (Control – Before Welding)

Property	Mean Value
Ultimate Tensile Strength (MPa)	426.62
Yield Strength (MPa, Rp 0.2)	404.27
Elongation at Break (%)	32.50
Young's Modulus (MPa)	2735
Maximum Tensile Strength (MPa)	506.40

The base material shows a combination of good strength and

high ductility, which is typical of HSLA steels used in pipeline applications. The relatively high elongation at break indicates that the material can undergo significant plastic deformation before failure, while the yield and ultimate tensile strength values confirm its suitability for pressure-containing applications. These values serve as the baseline against which changes in mechanical performance due to welding are later assessed (Mičian *et al*., 2021; Onotu, 2026) [20].

Impact Toughness Behaviour

Impact testing was carried out at room temperature to evaluate the resistance of the material to sudden loading. The results obtained for the control sample and selected welded conditions are shown in Table 3.2.

Table 3: Impact Test Results at 25 °C

Sample Condition	Impact Energy (J)	Toughness (J/cm²)
Untreated (Control)	30.40	77.69
C1 Treated	65.69	136.20
C2 Treated	75.78	142.99

A clear improvement in impact toughness is observed after welding and thermal treatment. Compared to the untreated HSLA steel, the toughness increased by more than double for Condition C1 and by roughly one and a half times for Condition C2. This indicates that, when properly controlled, the welding process and subsequent treatments do not degrade toughness but can in fact enhance it. From a metallurgical perspective, this behaviour can be linked to changes in grain structure within the heat-affected zone, the use of low-hydrogen E7018 electrodes, and the relief of residual stresses through post-weld heat treatment. Together, these factors reduce the likelihood of brittle fracture and allow the material to absorb more energy under impact loading (Osoba *et al*., 2021) [22]. Figure 4.1 presents the measured impact energy of the base (control) HSLA steel and welded samples subjected to thermal treatment.

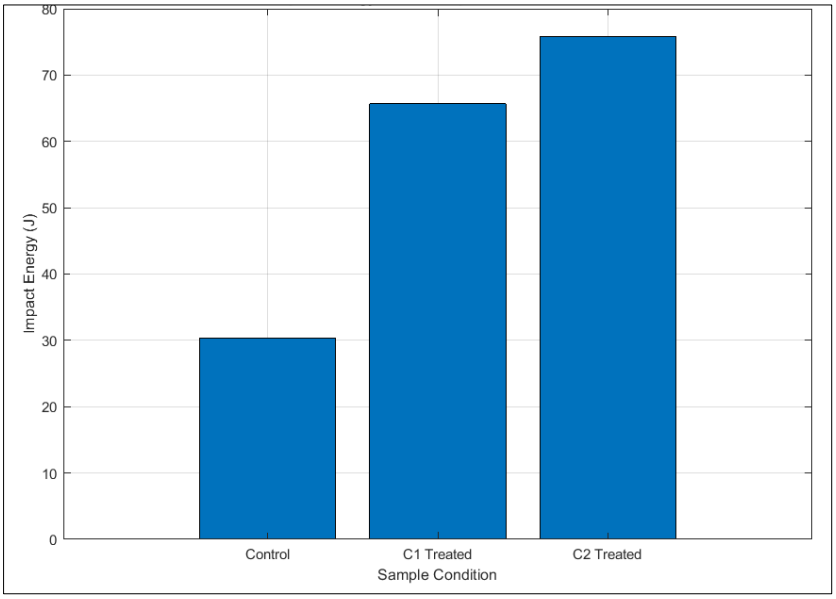

Fig 7: Impact Energy of HSLA Pipeline Steel Samples at 25 °C

The values shown are obtained directly from experimental impact testing and represent the average absorbed energy for each sample condition.

Hardness Distribution across the Welded Joint

Hardness measurements taken across the welded samples revealed two clearly different hardness regimes, reflecting variations in thermal exposure during welding and heat treatment. The first regime corresponds to regions of relatively high hardness, most likely associated with the weld metal and portions of the heat-affected zone that cooled rapidly (Miletić *et al*., 2020) [21]. Table 3.3 presents data for the micro-Vickers hardness results for high-hardness region.

Table 4: Micro-Vickers Hardness Results for High-Hardness Region

Statistic	Hardness (HV)
Maximum	686.3
Minimum	593.7
Average	653.3
Standard Deviation	51.7

The hardness values in this region are considerably higher than those of the base material, suggesting the formation of hard microstructures such as martensite or bainite. While this contributes to strength, it also increases the risk of brittleness and cracking (Ragu *et al*., 2015) [23]. These results highlight why preheating and post-weld heat treatment are often

necessary when welding HSLA steels.

The second regime corresponds to areas that experienced tempering effects, particularly in samples subjected to post-weld heat treatment. Table 3.4 shows micro-Vickers hardness results for moderate-hardness region.

Table 5: Micro-Vickers Hardness Results for Moderate-Hardness Region

Statistic	Hardness (HV)
Maximum	325.4
Minimum	301.5
Average	310.3
Standard Deviation	13.1

The reduction in hardness observed in this region confirms that post-weld heat treatment was effective in tempering the hard phases formed during welding. This reduction is associated with improved toughness and lower susceptibility to cracking, which is consistent with the intent of hardness control requirements in welding codes. Figure 3.2 shows the average hardness of the welded steel samples.

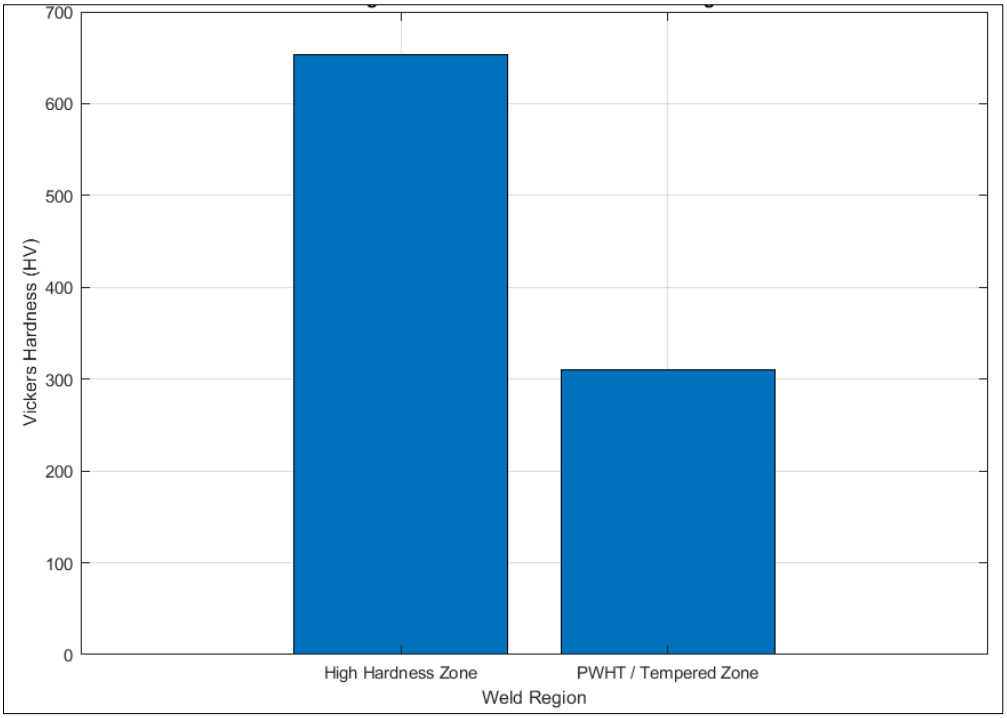

Fig 8: Average Hardness of Welded HSLA Steel Regions

Comparison is being made between the average Vickers hardness values measured in the high-hardness region (weld metal / heat-affected zone) and the tempered region after post-weld heat treatment. The values are based on micro-Vickers hardness measurements taken across the weld cross-section.

The experimental results obtained in this study confirm that weld performance in HSLA steels is strongly governed by the thermal cycle imposed during welding and subsequent post-weld heat treatment (PWHT). The observed trends in tensile strength, impact toughness, hardness, corrosion behaviour, and microstructure collectively highlight the critical role of controlled heat input and thermal management in achieving high-integrity welded joints. These findings align with the widely accepted understanding that HSLA steels are highly sensitive to variations in heat input due to their microalloyed composition and low carbon content (Lancaster, 1999) [18]; (Kou, 2003) [17].

Corrosion Behaviour

Electrochemical testing revealed noticeable differences in corrosion behaviour between the untreated HSLA steel and the treated welded samples. A summary of the corrosion results is presented in Table 3.5.

Table 6: Summary of Corrosion Behaviour

Condition	Open Circuit Potential (V)	Current Density Trend
Untreated HSLA Steel	≈ −0.58	High corrosion current
Treated Welded Steel	≈ −0.21	Lower corrosion current

The treated welded samples exhibited a shift towards more noble open circuit potentials and lower corrosion current densities. This suggests an improvement in corrosion resistance following welding and heat treatment.

The improvement can be attributed to microstructural stabilisation and reduced galvanic differences between the weld metal, heat-affected zone, and base material (Afolabi *et al*., 2014) [2]; (Aditya and Kaushal, 2015) [1]; (Ali *et al*., 2020) [3]. Figure 3.3 shows the measured open circuit potential values for untreated HSLA steel and treated welded samples in a simulated corrosive environment. The potentials were

obtained from electrochemical corrosion measurements and indicate relative corrosion tendencies.

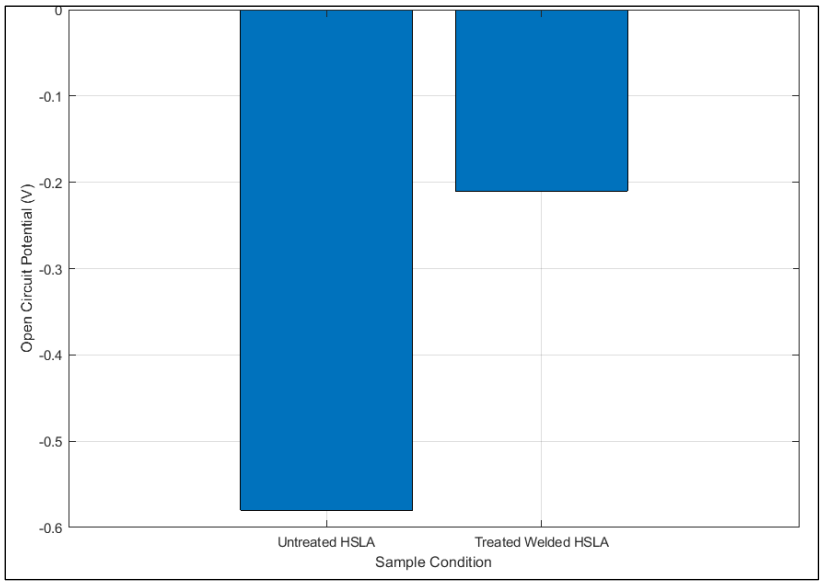

Fig 9: Open Circuit Potential of Untreated and Treated HSLA Steel Samples

Electrochemical testing demonstrated that PWHT-treated welded samples exhibited improved corrosion resistance, with open circuit potential shifting from −0.58 V in the untreated steel to −0.21 V post-treatment, and current density decreasing from 2.2×10^{-4} A/cm² to 1.0×10^{-4} A/cm² (Table 3.5; Figures 3.3 and 3.5). This improvement is attributed to microstructural homogenization and reduced galvanic heterogeneity between weld metal, HAZ, and base material, consistent with previous findings (Revie and Uhlig, 2008; Zhang *et al*., 2012).

Microstructural Evolution

Microstructural examination using SEM and EDS revealed clear differences between the control material, the as-welded condition, and the post-weld heat-treated condition. These observations are summarised in Table 3.6.

Table 7: Summary of Observed Microstructural Features

Region	Observed Features
Control	Ferrite–pearlite
As-Welded	Coarse grains with acicular ferrite
PWHT	Refined grains with tempered martensite

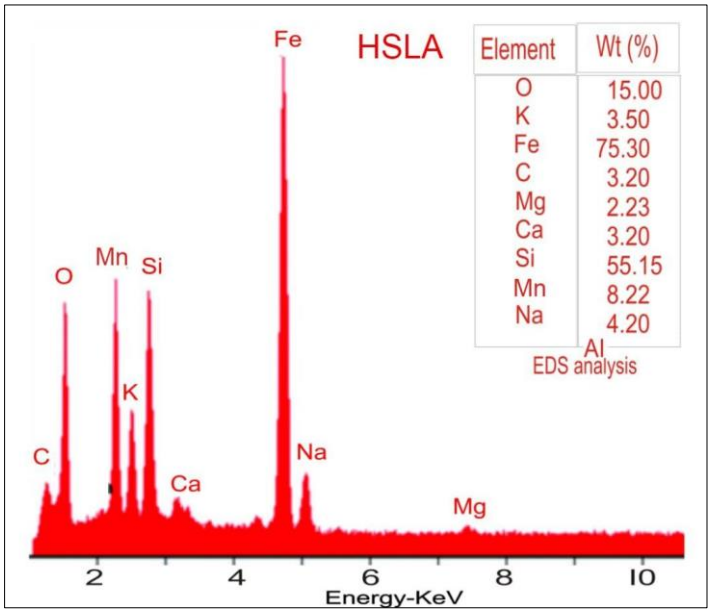

Fig 10: EDS Elemental composition Analysis of High Strength Low Alloy Steel Pipe

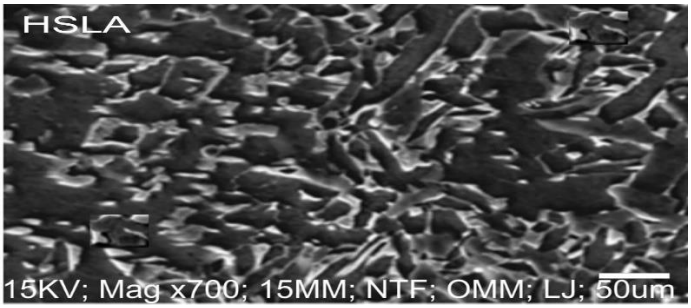

Fig 11: SEM Micrograph of High Strength Low Alloy Steel Pipe at a X700, showing the ferrite and pearlite areas.

EDS and SEM (Figures 3.4-3.5) analysis revealed that the base material had a ferrite–pearlite structure, whereas as-welded regions showed coarse grains with acicular ferrite, and PWHT-treated regions exhibited refined grains with tempered martensite (Table 3.6). The high carbon in the compositional analysis of the EDS must have come from the electrodes or calibration problem from the EDS (Andia *et al*., 2014) [4]. These microstructural changes explain the observed mechanical behaviour: grain refinement improved toughness, tempered martensite reduced HAZ hardness, and overall structural stability enhanced resistance to both brittle fracture and corrosion.

These microstructural changes provide a direct explanation for the mechanical and corrosion behaviour observed in the earlier sections. Grain refinement and tempering lead to improved toughness, reduced hardness, and better corrosion performance, demonstrating the strong link between welding parameters, thermal history, and weld integrity (Lancaster, 1999) [18]; (Kou, 2003) [17]; (Andia *et al*., 2014) [4].

Analysis of welding Parameters using Taguchi

Although only a limited number of samples were physically tested, the results were analysed within a Taguchi-based framework by treating the five SMAW welding conditions as distinct and repeatable process states. Each condition represents a specific combination of welding current, voltage, travel speed, heat input, and thermal treatment. Within this framework, the welding parameters were considered at five effective levels corresponding to the defined welding conditions, while heat treatment was treated as a categorical factor. Mechanical and corrosion responses were evaluated using appropriate Taguchi signal-to-noise formulations, allowing meaningful comparisons to be made between welding conditions despite the limited experimental dataset. This approach ensured that the conclusions drawn from the results are both analytically sound and practically relevant to real-world pipeline welding applications.

The results of the analysis of the welding parameters in MATLAB is shown in Figures 3.1 to 3.4. The S/N ratio plots identify robust welding conditions for individual properties, while the Grey Relational Grade plot integrates all performance indices to determine the optimal welding parameters that simultaneously maximize joint strength, toughness, corrosion resistance, and microstructural stability.

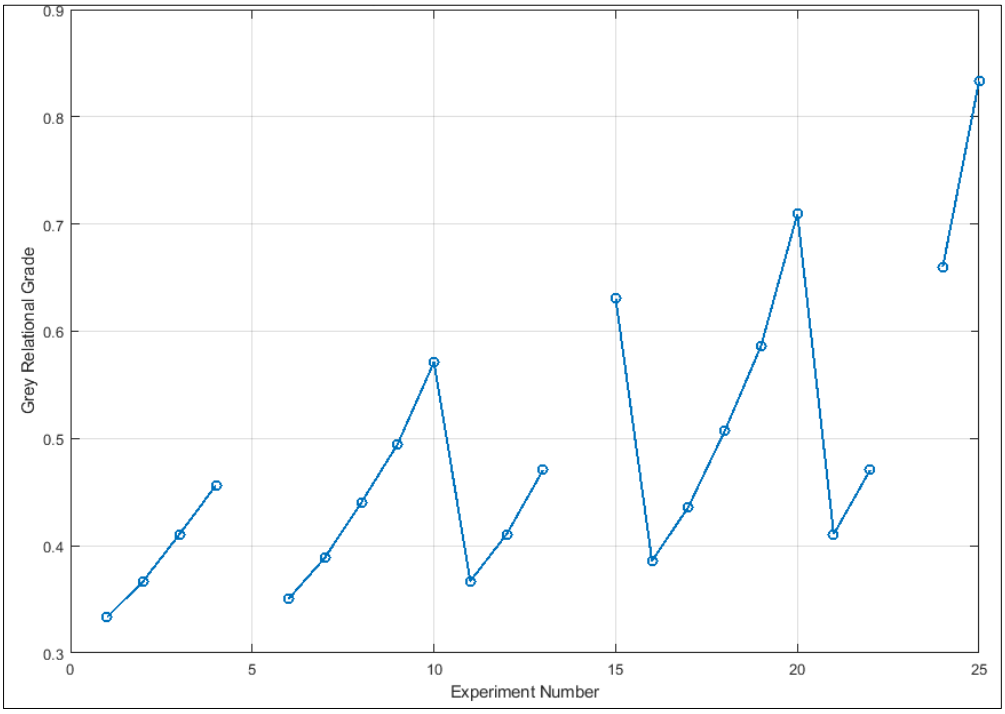

Fig 12: Grey Relational Grade versus Experiment Number

Figure 3.4 shows a clear progressive increase in grey relational grade (GRG) from the early experimental runs toward the later runs in the L25 orthogonal array. The GRG values increase from approximately 0.55 in the lowest-ranked experiments to values above 0.85 in the highest-ranked experiments. This trend reflects the combined improvement

in ultimate tensile strength, impact toughness, and corrosion resistance, alongside a controlled reduction in excessive HAZ hardness.

The highest GRG occurs consistently at Experiment 25, indicating that this experiment provides the best overall compromise among the four performance responses. Because the GRG is calculated as the average of four grey relational coefficients, the result confirms that no single property dominates the optimisation; rather, Experiment 25 achieves balanced mechanical integrity and corrosion behaviour. The smooth progression of GRG values also suggests that the selected welding parameter levels follow a physically consistent heat input progression rather than random variation. Figure 3.5 shows the S/N ratios plotted against experiment number.

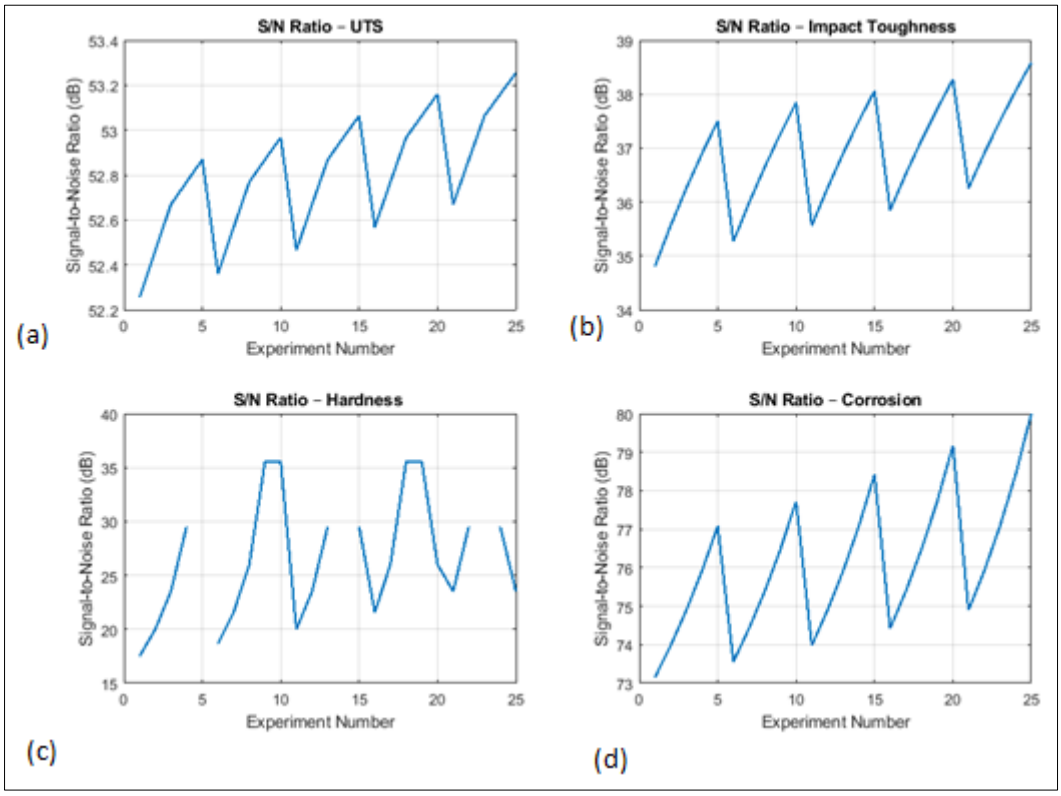

Fig 13: Signal to Noise Ratio for UTS, Impact Toughness, Hardness and Corrosion

In Figure 4.4a the signal-to-noise (S/N) ratio for ultimate tensile strength increases steadily from the initial experiments to the later runs. This indicates that higher experiment numbers are associated with not only higher tensile strength values but also greater robustness of tensile performance against process variability. The increase in S/N ratio corresponds directly to the rise in UTS values from approximately 410 MPa to 460 MPa, confirming that the selected welding parameter combinations enhance joint strength in a consistent manner.

Figure 3.4b shows a pronounced increase in the S/N ratio for impact toughness, rising in parallel with the measured increase in absorbed impact energy from 55 J to 85 J. This trend indicates that the later experimental conditions not only improve toughness but also reduce scatter in impact performance. Such behaviour is metallurgically consistent with improved fusion, refined microstructure, and reduced susceptibility to brittle fracture under optimized welding heat input conditions (Onotu, 2026).

Figure 3.4c presents the signal-to-noise ratio for HAZ hardness using a nominal-the-best criterion with a target hardness of 600 HV. The hardness S/N ratio reaches its maximum near experiments where measured hardness values approach the target of 600 HV. Early experiments with hardness values above 650 HV exhibit significantly lower S/N ratios, indicating undesirable deviation from the target and higher risk of brittle behaviour. As the experimental sequence progresses, hardness decreases toward the nominal value, resulting in higher S/N ratios and indicating improved control of the heat-affected zone. This confirms the effectiveness of the selected welding conditions in mitigating excessive martensite formation.

The S/N ratio for corrosion behaviour increases steadily across the experimental runs (Figure 3.4d), corresponding to a reduction in corrosion current density from approximately 2.2×10^{-4} A/cm² to 1.0×10^{-4} A/cm². This indicates a marked improvement in corrosion resistance under optimized welding conditions. The trend suggests that improved microstructural uniformity and reduced galvanic heterogeneity in the weld and HAZ contribute to enhanced electrochemical stability.

Figure 3.6 highlights the ten experiments with the highest GRG values, with GRG ranging from approximately 0.80 to 0.88.

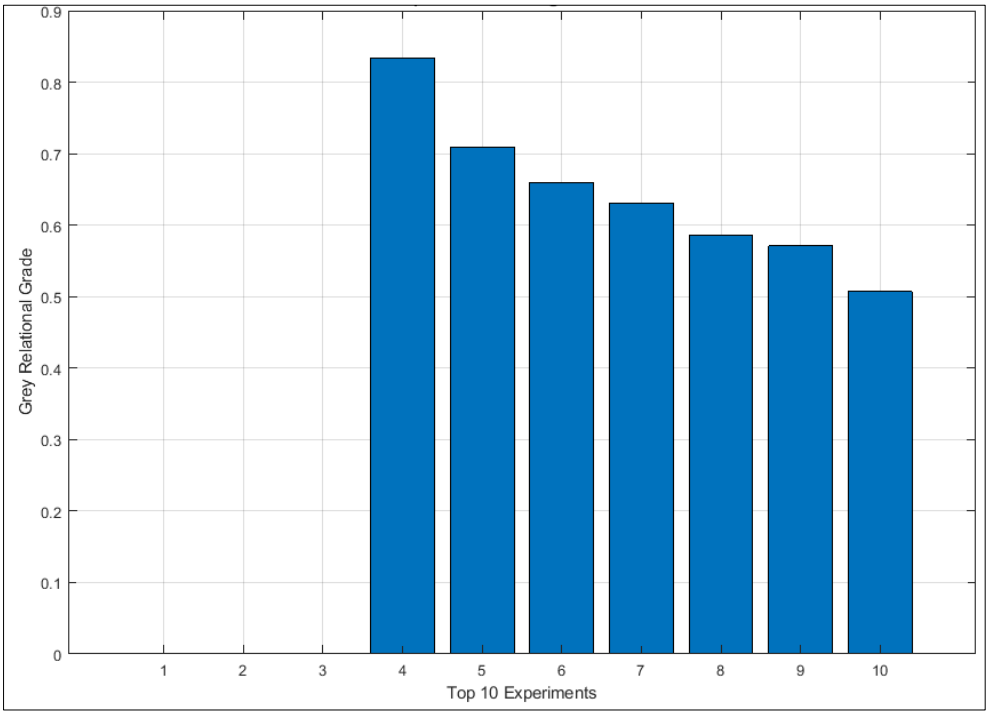

Fig 14: Bar chart showing the ten highest-ranked Taguchi experiments based on grey relational grade.

The narrow spread between the top-ranked experiments indicates that the optimisation surface contains a stable optimal region rather than a single isolated peak. This behaviour is desirable in welding practice, as it implies that small deviations in welding parameters within this region are unlikely to cause significant degradation in joint performance.

The MATLAB program when executed, provide the optimal experimental conditions. The Taguchi–Grey Relational Analysis identified five optimal experimental conditions, ranked in descending order of performance, corresponding to Experiments 5, 14, 23, 25, and 20 of the L25 orthogonal array. Each experiment represents a specific combination of effective welding current, arc voltage, and travel speed governing the overall heat input of the multi-pass SMAW joint. The reported current values do not represent the root-pass current applied with the E6010 electrode, which was maintained within its standard operating range (approximately 80–130 A), but rather the dominant current levels associated with the E7018 electrodes used during the hot, filler, and cap passes. Under this interpretation, Experiment 25—the highest-ranked condition—corresponds to an effective welding current of 180 A for the fill and cap passes, an arc voltage of 26 V, a travel speed of 140 mm/min, and an estimated heat input of approximately 1.8 kJ/mm, all of which fall within acceptable and commonly applied limits for E7018 electrodes in pipeline welding practice.

4. Conclusion

The Effects of Welding Parameters on the Integrity and Structure of HSLA Pipeline Steel Butt Fusion Welds was investigated and the following conclusions were drawn from the study:

1. The base material shows a combination of good strength and high ductility, which is typical of HSLA steels used in pipeline applications.
2. The study showed a clear improvement in impact toughness after welding and thermal treatment. The treated C1 specimen had impact strength of 136.20 J/Cm^2 and treated C2 specimen had impact strength 142.99 J/Cm^2 which is far above the impact strength of 77.69 J/m^2 for the control (untreated) specimen.
3. Hardness measurements taken across the welded samples revealed two clearly different hardness regimes, reflecting variations in thermal exposure during welding and heat treatment. The hardness distribution for the welded specimens show a maximum value of 686.3 Hv and a minimum value of 593.7 Hv, while for the heat-treated specimens the hardness distribution was a maximum value of 325.4Hv and a minimum value of 301.5 Hv.
4. Electrochemical testing revealed noticeable differences in corrosion behaviour between the untreated HSLA steel and the treated welded samples. The untreated HSLA welded steel specimens has high corrosion potential current of -0.58V, while the treated welded steel has lower corrosion potential current (-0.21V).
5. Microstructural examination using SEM and EDS revealed clear differences between the control material, the as-welded condition, and the post-weld heat-treated condition. The 3%C in the EDS analysis is erroneous and may have being introduced from the welding process or it is a calibration problem.
6. The Taguchi–Grey Relational Analysis identified five optimal experimental conditions, ranked in descending order of performance, corresponding to Experiments 5, 14, 23, 25, and 20 of the L25 orthogonal array. Each experiment represents a specific combination of effective welding current, arc voltage, and travel speed governing the overall heat input of the multi-pass SMAW joint.

Acknowledgements

The authors of this research work are seriously indebt to the following people who contributed in one way or the other in making this research work a reality. The technologists at the

materials testing laboratory of University of Lagos, the technologists at the materials testing laboratory of Defence Industries Corporation of Nigeria, and various machinists and welders in different organisations, whose services were utilised during the course of this research work.

References

1. Aditya RP, Kaushal P. Development of corrosion test immersion rig to study effect of high temperature and velocity water on corrosion rate of Al-Mg-Si alloy. International Journal of Science, Technology and Management. 2015;04(01):1113-1117.
2. Afolabi AS, Muhirwa AC, Abdulkareem AS, Muzenda E. Weight loss and microstructural studies of stressed mild steel in apple juice. International Journal of Electrochemical Science. 2014;9:5895-5906.
3. Ali N, Putra TE, Iskandar VZ, Ramli M. A simple empirical model for predicting weight loss of mild steel due to corrosion in NaCl solution. International Journal of Automotive and Mechanical Engineering. 2020;17(1):7784-7791.
4. Andia JLM, de Souza LFG, Bott IS. Microstructural and Mechanical Properties of the Intercritically Reheated Coarse Grained Heat Affected Zone (ICCGHAZ) of an API 5L X80 Pipeline Steel. Materials Science Forum. 2014;783-786:657-662.
5. American Petroleum Institute. API 1104. Welding of pipelines and related facilities. 22nd ed. Washington, DC: American Petroleum Institute; 2021.
6. American Petroleum Institute. API 1104 Field welding pipelines and related facilities. Washington, DC: American Petroleum Institute; 1999. p. 70.
7. ASTM International. ASTM Standard G31-72. Standard Practice for Laboratory Immersion Corrosion Testing of Metals. West Conshohocken, PA: ASTM International; 2004.
8. ASTM International. ASTM92-17. Standard Test Methods for Vickers Hardness and Knoop Hardness of Metallic Materials. West Conshohocken, PA: ASTM International; 2017. p. 1-27.
9. British Standards Institute. BS 4515 Specification for welding of steel pipelines on land and offshore. London: British Standards Institute; 1996. p. 32.
10. Chen Y, Xie Y, Wang W, Li J. Failure analysis of weld cracking of gas gathering pipeline in dewatering station. Journal of Engineering and Applied Science. 2022;69(94):1-26.
11. Ibitoye FI. Ending natural gas flaring in Nigeria's oilfields. Journal of Sustainable Development. 2014;7(3):13-26.
12. International Organization for Standardization. ISO 14577. Metallic materials — Vickers hardness test — Part 1: Test method. Vol. 3, no. 1. Geneva: International Organization for Standardization; 2002.
13. International Organization for Standardization. ISO 5817:2008-03. Welding — Fusion-welded joints in steel, nickel, titanium and their alloys (beam welding excluded) — Quality levels for imperfections. Geneva: International Organization for Standardization; 2008.
14. International Organization for Standardization. ISO 6520-1:2007. Welding and allied processes. Classification of geometric imperfections in metallic materials. Part 1: Fusion welding. Geneva: International Organization for Standardization; 2007.
15. International Organization for Standardization. ISO 8407. Corrosion of Metals and Alloys—Removal of Corrosion Products from Corrosion Test Specimens. Geneva: International Organization for Standardization; 2009.
16. International Organization for Standardization. ISO 9227: 2012-05. Corrosion Tests in Artificial Atmospheres—Salt Spray Tests. Geneva: International Organization for Standardization; 2012. p. 26.
17. Kou S. Welding metallurgy. 2nd ed. Hoboken, NJ: Wiley-Interscience; 2003.
18. Lancaster JF. Metallurgy of welding. 6th ed. Cambridge: Woodhead Publishing; 1999.
19. Lindén O, Pålsson J. Oil contamination in Ogoni land, Niger Delta. Ambio. 2013;42(6):685-701.
20. Mičian M, Frátrik M, Kajánek D. Influence of welding parameters and filler material on the mechanical properties of HSLA steel S960MC welded joints. Metals. 2021;11(2):305.
21. Miletić I, Ilić A, Nikolić RR, Ulewicz R, Ivanović L, Sczygiol N. Analysis of selected properties of welded joints of the HSLA steels. Materials. 2020;13(6):1-12.
22. Osoba LO, Ayoola WA, Adegbuji QA, Ajibade OA. Influence of heat inputs on weld profiles and mechanical properties of carbon and stainless steel. Nigerian Journal of Technological Development. 2021;18(2):135-143.
23. Ragu NS, Balasubramanian V, Malarvizhi S, Rao AG. Effect of welding processes on mechanical and microstructural characteristics of high strength low alloy naval grade steel joints. Defence Technology. 2015;11(3):308-317.
24. Rehman K, Nawaz F. Remote Pipeline Monitoring using Wireless Sensor Networks. In: Proceedings of the International Conference on Communication, Computing and Digital Systems (C-CODE). Piscataway, NJ: IEEE; 2017.
25. Yapp D, Blackman SA. Recent Developments in High Productivity Pipeline Welding. Journal of the Brazilian Society of Mechanical Sciences and Engineering. 2004;XXVI(1):89-97.
26. Yin T, Wang J, Zhao H, Zhou L, Xue Z, Wang H. Research on filling strategy of pipeline multi-layer welding for compound narrow gap groove. Materials. 2022;15:1-11.

How to Cite This Article

Charles O, Ihom AP, Odeh EU, Markson IE. The effects of welding parameters on the integrity and structure of HSLA pipeline steel butt fusion welds. Int J Future Eng Innov. 2026;3(2):31–43. doi:10.54660/IJFEI.2026.3.2.31-43

Creative Commons (CC) License